

Research Article

# Persistence of risk factors associated with maternal cardiovascular disease following aberrant inflammation in rat pregnancy<sup>†</sup>

Takafumi Ushida<sup>1,2</sup>, Shannyn K. Macdonald-Goodfellow<sup>1</sup>, Allegra Quadri<sup>1</sup>, M. Yat Tse<sup>1</sup>, Louise M. Winn<sup>1</sup>, Stephen C. Pang<sup>1</sup>, Michael A. Adams<sup>1</sup>, Tomomi Kotani<sup>2</sup>, Fumitaka Kikkawa<sup>2</sup> and Charles H. Graham<sup>1,\*</sup>

<sup>1</sup>Department of Biomedical and Molecular Sciences, Queen's University, Kingston, Ontario, Canada and <sup>2</sup>Department of Gynecology and Obstetrics, Nagoya University Graduate School of Medicine, Showa-ku, Nagoya, Japan

\*Correspondence: Department of Biomedical and Molecular Sciences, Botterell Hall, 18 Stuart Street, Kingston, Ontario K7L 3N6, Canada. E-mail: [grahamc@queensu.ca](mailto:grahamc@queensu.ca)

<sup>†</sup>Grant Support: This work was supported by a grant from the Canadian Institutes of Health Research (MOP119496) awarded to CHG.

Received 19 April 2017; Revised 12 June 2017; Accepted 4 July 2017

## Abstract

**Introduction:** Pre-eclampsia is associated with increased risk of subsequent cardiovascular and metabolic disease in the affected mothers. While aberrant inflammation contributes to the pathophysiology of pre-eclampsia, it is unclear whether maternal inflammation contributes to the increased risk of disease. Here, we determined the effect of aberrant inflammation in pregnancy on cardiovascular and metabolic disease risk factors.

**Methods:** Wistar rats were administered low doses of lipopolysaccharide (LPS) on gestational days (GD) 13.5–16.5 to induce inflammation. Controls included pregnant rats treated with saline and nonpregnant rats treated with LPS or saline. We previously showed that LPS-treated pregnant rats exhibit key features of pre-eclampsia. Echocardiographic parameters, heart weight, blood pressure, blood lipids, pulse-wave velocity, and glucose tolerance, were assessed at 16 weeks postpartum. Messenger RNA levels of transcription factors associated with cardiac growth were measured in left ventricular tissue; histone modifications and global DNA methylation were determined in hearts and livers at GD 17.5 and at 16 weeks postpartum.

**Results:** Compared with saline-treated pregnant rats and nonpregnant rats treated with LPS or saline, LPS-treated pregnant rats exhibited left ventricular hypertrophy and increased blood cholesterol and low-density lipoprotein levels at 16 weeks postdelivery. LPS-treated rats had increased left ventricular mRNA levels of hypertrophy-associated transcription factors at GD 17.5 and increased levels of modified histones in hearts and livers at GD 17.5 and 16 weeks postpartum. Other parameters remained unchanged.

**Conclusion:** Aberrant inflammation during pregnancy results in persistent alterations in maternal physiological parameters and epigenetic modifications that could contribute to the pathophysiology of cardiovascular disease.

## Summary Sentence

Abnormal inflammation during rat pregnancy leads to persistence of maternal risk factors for cardiovascular disease, including left ventricular hypertrophy and increased levels of cholesterol and low-density lipoprotein.

**Key words:** maternal inflammation, pre-eclampsia, intrauterine growth restriction, cardiac hypertrophy, hyperlipidemia, cardiovascular disease, epigenetics.

## Introduction

Certain complications of pregnancy, such as pre-eclampsia, intrauterine growth restriction (IUGR), and preterm birth, are associated with an increased risk of cardiovascular disease in later life for the affected mothers and their offspring [1–3]. Women and children affected by pre-eclampsia are more likely to develop metabolic syndrome [4, 5], a condition characterized by insulin resistance, obesity, hypertriglyceridemia, low high-density lipoprotein (HDL) cholesterol, hypertension, and dysglycemia; all significant risk factors for cardiovascular disease [6]. The concept of Developmental Origins of Health and Disease pioneered by David Barker postulates that the fetus undergoes adaptive responses (i.e., programming) in an attempt to improve in utero survival during complicated pregnancies [7]. However, after birth and later in life, these responses may be maladaptive, resulting in increased blood levels of cholesterol, hypertension, left ventricular hypertrophy, and diabetes; each increasing the risk of cardiovascular and metabolic disease [8, 9]. Similarly, it is now known that pre-eclampsia also increases the risk of developing chronic hypertension in the mother, with a risk as high as 38% within 13 years of the affected pregnancy [2], and more than half of women with preterm pre-eclampsia have a higher incidence of left ventricular dysfunction or hypertrophy postpartum [10]. Women with a previous pregnancy complicated by early-onset pre-eclampsia had significantly higher fasting blood glucose levels as well as increased insulin, triglycerides (TG), and total cholesterol (TC) levels than women previously afflicted by a late-onset pre-eclamptic pregnancy [11]. Furthermore, 21% of women who suffer from severe pre-eclampsia on a first pregnancy develop severe pre-eclampsia in a subsequent pregnancy [12], and daughters born to pre-eclamptic women have more than twice the risk of developing pre-eclampsia themselves [13]. Thus, complications such as IUGR and pre-eclampsia represent a significant health risk for mothers and their children, not only during pregnancy but also in subsequent years and across generations. Developing interventions to reduce the incidence or severity of these diseases will be of substantial health benefit, as current treatments address only the symptoms of IUGR/pre-eclampsia and fail to alter the underlying pathophysiology [14].

Aberrant maternal inflammation during pregnancy is often linked to the etiology of IUGR and pre-eclampsia [15–19]. Many women with IUGR and/or pre-eclampsia have a heightened inflammatory state characterized by high levels of circulating proinflammatory molecules [17, 19, 20]; and severely pre-eclamptic women may suffer from disseminated intravascular coagulation with widespread microvascular occlusive thrombi leading to renal and liver failure, placental and cerebral infarction, and seizures [14, 21]. IUGR and pre-eclampsia are also linked to abnormal activation of uterine leukocytes [22, 23]. For instance, macrophages are aberrantly activated in pre-eclampsia [23, 24], and mediate fetal demise in a mouse model [25]. High levels of macrophage chemotactic factors are secreted by the placental endothelium of pregnancies complicated by IUGR and pre-eclampsia [26]. Also, in IUGR and pre-eclampsia,

there are large numbers of macrophages present around the uterine spiral arteries [23]; these macrophages secrete tumor necrosis factor- $\alpha$  (TNF) at levels that cause apoptosis of the invading trophoblasts, thereby preventing the remodeling of the spiral vessels that is required for adequate placentation [27]. Maternal circulating levels of immunoregulatory molecules such as human leukocyte antigen-G (HLA-G), pregnancy-specific glycoproteins, prostaglandin E<sub>2</sub>, annexin V, interleukin (IL) 4, IL5, and IL10 are decreased in IUGR and pre-eclampsia compared with uncomplicated pregnancies [15, 28].

To determine a causal link between inflammation and the development of pregnancy complications, we previously established a model of IUGR and pre-eclampsia in which inflammation is induced in pregnant Wistar rats by low-dose lipopolysaccharide (LPS) administration [29]. These rats develop features of pre-eclampsia, including elevated blood pressure, proteinuria, renal abnormalities, deficient trophoblast invasion of the endometrium, impaired spiral artery remodeling, placental hemodynamic alterations, placental oxidative stress, local and systemic coagulopathies, and IUGR [29, 30]. Interestingly, a similar dose of LPS given to nonpregnant rats did not induce a detectable inflammatory response, hypertension, proteinuria, or renal abnormalities [29], indicating that pregnancy amplifies inflammatory stimuli resulting in complications. This concept is supported by studies showing that women with underlying conditions involving chronic inflammation, such as obesity, periodontal disease, diabetes, chronic hypertension, and bacterial or viral infections, have a higher risk of developing pre-eclampsia or preterm birth [31, 32]. It has been proposed that cardiovascular/metabolic risk factors present prior to gestation are required for the development of pregnancy complications such as pre-eclampsia, and that these risk factors persist after the affected pregnancies to trigger subsequent disease [33]. On the contrary, it is also possible that in some circumstances, even without pre-existing risk factors, pregnancy complications could disrupt maternal homeostasis, thereby increasing the risk of disease later in life. In support of this concept, Pruthi et al. recently demonstrated persistent vascular alterations in mice exhibiting a pre-eclampsia-like condition as a result of overexpression of soluble fms-like tyrosine kinase-1 (sFlt-1) [34]. Also, a recent study revealed that a reduction in the number of circulating endothelial progenitor cells in pregnancy may affect long-term endothelial function [35].

While there is evidence for a causal link between abnormal inflammation and the development of pregnancy complications such as pre-eclampsia, it is still not clear whether the subsequent risk of maternal cardiovascular disease is a consequence of abnormal inflammation during the affected pregnancies. Knowledge of such mechanistic association could provide insight into the development of strategies aimed at preventing serious complications of pregnancy and, consequently, decreasing the incidence of subsequent disease. In the present study, using a rat model, we provide evidence that induction of aberrant maternal inflammation during pregnancy results in persistent alterations associated with risk of cardiovascular disease as well as epigenetic modifications in the heart and liver.

## Materials and methods

### Animal model

This study was conducted in accordance with the guidelines of the Canadian Council on Animal Care and the Society for the Study of Reproduction; all protocols were approved by the Queen's University Animal Care Committee. Virgin female Wistar rats (12–16 weeks of age) and male Wistar rats were purchased from Charles River Laboratories (Montreal, QC, Canada). Rats were housed in a temperature-controlled room under a 12-h light/dark cycle and were provided a standard diet and tap water ad libitum. Virgin rats were mated overnight with males at a 2:1 ratio. The following morning, the presence of spermatozoa in the vaginal lavage confirmed pregnancy and was designated gestational day (GD) 0.5. Pregnant rats were randomly divided in saline- and LPS-treated groups. Additional controls consisted of nonpregnant rats treated with LPS or saline. The LPS-treated experimental group (pregnant) received intraperitoneal (i.p.) injections of LPS (*Escherichia coli* serotype 0111:B4; Sigma-Aldrich, Oakville, ON, Canada) on GD 13.5 (10 µg/kg) and on GDs 14.5–16.5 (40 µg/kg/day). Control rats received saline (1 ml/kg/day) injections on GDs 13.5–16.5. Nonpregnant rats received a similar 4-day injection protocol of LPS or saline. Rats received 5 ml of subcutaneous injection of lactated Ringer solution with each i.p. injection. Half of the pregnant rats were sacrificed on GD 17.5 under anesthesia with sodium pentobarbital (Ceva Santé Animale, Libourne, France). Serum samples and maternal organs were collected for subsequent assays. The other half of pregnant rats was allowed to deliver. To eliminate potential variability in maternal outcomes due to differential litter sizes, the number of pups from each litter was culled to eight (four male and four female pups per litter) on postnatal day (PND) 1 and weaned from their respective mothers at PND 21.

### Blood glucose monitoring and intraperitoneal glucose tolerance test

Fasting blood glucose levels were measured from tail vein blood using a One Touch Ultra 2 glucose monitoring system (Life Scan, Burnaby, BC, Canada), after overnight (14–16 h) fasting, every 4 weeks after delivery. Intraperitoneal glucose tolerance test (IPGTT) was performed once after overnight fasting and at 16 weeks postpartum. A 20% glucose solution (2 g/kg body weight) was injected i.p., and blood glucose levels were measured at 0, 15, 30, 60, 90, and 120 min after glucose administration.

### Echocardiography

Echocardiographic examination was performed to assess cardiac structure and function using a Vevo 2100 ultrasonography machine (VisualSonics, Toronto, ON, Canada) at 16 weeks postpartum. Anesthesia was induced using 5% isoflurane in oxygen and maintained with continuous 2–3% isoflurane ventilation by nose cone. Maternal heart and breathing rates were monitored throughout the study. Cardiac scans were performed using a 21 MHz MicroScan transducer (MS-250, VisualSonics). Left ventricular systolic and diastolic functions were measured in parasternal long axis and apical four-chamber view by M-Mode, color Doppler Mode, and tissue Doppler Mode. Ultrasound data were analyzed using Vevo Lab software (VisualSonics).

### Blood pressure and pulse-wave velocity

Blood pressure and pulse-wave velocity (PWV) were measured as previously described [36]. Sixteen weeks after delivery, all rats were anesthetized via isoflurane inhalation. A single pressure catheter was inserted through the left carotid artery into the descending aorta to measure proximal aortic blood pressure. Another catheter was inserted into the lower abdominal aorta through the left femoral artery to measure distal aortic blood pressure. Proximal and distal aortic blood pressure signals were simultaneously monitored and recorded via an attached pressure transducer (Transonic SP200 pressure system, Ithaca, NY, USA). After measurement of blood pressure, the tips of the two catheters were visually marked, and the distance between the two points was measured. Rats were euthanized and tissues were collected, and stored at –80°C for later analysis. PWV provides an indication of arterial wall stiffness. It was calculated as the aortic distance between the two catheters divided by the wave transmission time using LabChart8 analysis software (ADInstruments, Colorado Springs, CO, USA). At least 100 normal waveforms were individually analyzed and averaged. To reduce the influence of blood pressure on PWV, especially diastolic pressure,  $\beta$  index was calculated according to the formula  $2.11 \times (\text{PWV}^2/\text{diastolic pressure})$  [37].

### Complete blood cell count and analysis of serum lipids and renal function

Complete blood cell (CBC) count and serum analysis was performed at 16 weeks postpartum at the time of euthanasia. CBC count analysis was performed using ABC Vet Animal Blood Counter (Scil Animal Care Company, Gurnee, IL, USA) according to the manufacturer's instructions. Serum samples were assessed for TC, HDL cholesterol, TG, creatinine, and urea by the Core Laboratory at Kingston General Hospital. Low-density lipoprotein (LDL) cholesterol was calculated by the following formula:  $\text{TC} - [\text{TG}/5 + \text{HDL cholesterol}]$ .

### Cardiac histology

Heart tissue samples were fixed in 10% formalin, dehydrated in graded series of ethanol, embedded in paraffin, and 5-µm serial sections were cut using a Leica RM2125 RTS microtome (Wetzlar, Germany). Sections were stained with hematoxylin and eosin (H&E) to determine the structure of cardiomyocytes, or were stained with Sirius red (0.1% Direct Red 80, Sigma-Aldrich, in 1% picric acid) and Masson trichrome (HT15, Sigma-Aldrich) to assess collagen content. In the cross and longitudinal sections stained with H&E, the area and width of cardiomyocytes in the left ventricle were quantified using a computerized image analysis system (ImageJ 1.48, W.S. Rasband, National Institutes of Health (NIH), Bethesda, MD). Percent fibrosis area was calculated in sections stained with Sirius red and Masson trichrome. Each analysis was conducted by a blinded observer.

### RNA isolation and real-time quantitative polymerase chain reaction (PCR)

Total RNA was extracted from tissues using a combination of Trizol (Tri Reagent, Molecular Research Centre, Burlington, ON, Canada) and a High Pure RNA Isolation Kit (Roche Scientific Co., Laval, QC, Canada) as described previously [38]. Equal amounts of RNA (1 µg) were reverse transcribed to generate cDNA using a High-Capacity RNA-to-cDNA Kit (Thermo Fisher Scientific, Burlington, ON, Canada). Real-Time PCR was performed using a LightCycler 480 system II (Roche Scientific), and FastStart SYBR Green Master (Roche Scientific). Primers were designed using Primer Design 2.01

software (Scientific & Educational Software, Cary, NC, USA) from published mRNA sequences from the NIH GenBank. Sequences of each primer set (natriuretic peptide type A, *Nppa*; natriuretic peptide type B, *Nppb*; GATA binding protein 4, *Gata4*; GATA binding protein 6, *Gata6*; E1A binding protein p300, *Ep300*; myocyte enhancer factor 2C, *Mef2c*) are outlined in Supplementary Table S1. The PCR conditions were as follows: denaturation at 95°C for 5 min, followed by 40–50 cycles at 95°C for 20 s, 59°C for 15 s, and 72°C for 15 s. The expression of each gene was normalized according to  $\beta$ -actin expression.

### Determination of histone modifications

As previously described [39], tissues were homogenized on ice in Triton extraction buffer [phosphate buffered saline (PBS) containing 0.5% Triton X 100 (v/v), 2 mM phenylmethylsulfonyl fluoride, 0.02% sodium azide (w/v)], washed, and suspended in 0.2 N HCl overnight at 4°C. Supernatants were collected and protein concentrations were quantified using the BioRad protein assay (5000–002JA, Bio-Rad Laboratories, Mississauga, ON, Canada). Equal amounts of histones (5  $\mu$ g for liver, kidney, and pancreas; 15  $\mu$ g for heart) were prepared by boiling samples in loading buffer composed of 90% Laemmli sample buffer and 10% 1 M dithiothreitol (DTT). The separation of histones was performed by sodium dodecyl sulfate polyacrylamide gel electrophoresis (SDS-PAGE) on 15% polyacrylamide gels followed by transfer to polyvinylidene fluoride (PVDF) membranes. Membranes were blocked in 5% skim milk for 1 h, and then incubated with either antihistone H3 antibody or antihistone H4 antibody (1:5000 dilution; Merck Millipore Corporation, Etobicoke, ON, Canada) overnight. Membranes were incubated with appropriate secondary antibodies and visualized using enhanced chemiluminescence. X-ray film was used for capturing luminescent signals. Membranes were then stripped by incubating in stripping solution (Restore PLUS Western Blot Stripping Buffer, Thermo Fisher) for 15 min and reprobed with either antiacetyl-histone H3 or antiacetyl-histone H4 (1:5000 dilution; Merck Millipore Corporation), or with antimonomethyl-histone H3K9 (1:1000 dilution; Abcam, Toronto, ON, Canada) overnight. ImageJ software was used to measure the relative optical densities of the bands.

### Quantification of global DNA methylation

Total DNA was isolated from tissues using the DNeasy Blood & Tissue Kit (Qiagen, Montreal, QC, Canada) according to the manufacturer's instructions. DNA quality was assessed by photometric measurement of ratios 260/280 nm and 260/230 nm using a NanoDrop 2000 spectrometer (Thermo Scientific, Wilmington, DE, USA). DNA samples (100 ng) were quantified for global methylation by specifically measuring levels of 5-methylcytosine (5-mC) using the MethylFlash Global DNA Methylation (5-mC) enzyme-linked immunosorbent assay (ELISA) Easy Kit (Epigentek, Canada).

### Data and statistical analysis

Statistical analysis was performed using GraphPad Prism 7.0 software (GraphPad software Inc., La Jolla, CA, USA). Distribution and variation were evaluated by means of the Shapiro–Wilk test and the Levene test, respectively. To compare two groups, the Student's *t*-test and Mann–Whitney test were performed for parametric and non-parametric distributions, respectively. Food intake and glucose tolerance assessments were analyzed by repeated measures two-way analysis of variance (ANOVA). All data are expressed as mean  $\pm$  standard error of the mean (SEM). A value of  $P < 0.05$  was considered statistically significant.

## Results

### Inflammation in pregnancy induces cardiac hypertrophy

Assessment of heart weights/tibia length ratios revealed left ventricular hypertrophy (left ventricular weight/tibia length ratio) at 16 weeks postpartum in rats treated with LPS compared with saline-treated control rats (0.18 and 0.17, respectively,  $P < 0.01$ ; Figure 1A). While nonpregnant rats treated with LPS exhibited a trend toward left ventricular hypertrophy after 16 weeks, this effect of LPS was not significant ( $P = 0.10$ ). No significant difference was found in right ventricular, left atrium, and right atrium (Supplementary Figure S1A and B). Sections of left ventricles from LPS-treated rats stained with H&E, Masson trichrome, or Sirius red did not reveal overt histological differences compared with similar tissues from saline-treated rats (Figure 1B). Histological analysis revealed a nonsignificant trend toward decreased cardiomyocyte area ( $P = 0.26$ ) and width ( $P = 0.05$ ) in the LPS group (Figure 1C). Quantification of perivascular collagen fiber area, using Masson trichrome staining, and interstitial fibrosis area, using Sirius red staining, did not reveal significant differences between the LPS- and saline-treated groups (Figure 1C).

### Effect of maternal inflammation on cardiac hypertrophy-related gene expression

In order to gain further insight on the effect of LPS on cardiac hypertrophy, we determined the levels of expression of genes involved in cardiac hypertrophy. Exposure of rats to LPS on GDs 13.5–16.5 resulted in significant increases ( $P < 0.05$ ) in the cardiac mRNA levels of *Ep300* and *Mef2c* measured on GD 17.5 by qPCR (Figure 2E and F). Similarly, LPS-treated rats exhibited a trend ( $P = 0.06$ ) toward increased levels of *Gata6* mRNA, another transcription factor involved in cardiac growth (Figure 2D). The mRNA levels of *Gata4*, *Nppa*, and *Nppb* were not significantly different in control versus LPS-treated rats (Figure 2A–C). By 16 weeks postpartum, there were no significant differences in the mRNA levels of these transcription factors in heart tissues from control versus LPS-treated rats (Figure 2A–F).

### Effect of maternal inflammation on cardiac function

Mean arterial pressure as well as systolic and diastolic blood pressures were not significantly different in the LPS versus saline-treated rats at 16 weeks postpartum (Table 1); however, pulse pressure in the LPS treatment group was significantly decreased compared with the saline control group ( $32.2 \pm 1.3$  mmHg versus  $38.1 \pm 1.5$  mmHg, respectively,  $P < 0.05$ ; Table 1). Results of echocardiography, to evaluate systolic and diastolic function, did not reveal significant differences between the two groups. Similarly, results of PWV measurements to evaluate aortic wall stiffness did not reveal significant differences between the two groups even following normalization using  $\beta$  index.

### Effect of maternal inflammation on circulating lipids, visceral fat, body weight, food consumption, and glucose metabolism

Circulating TC and LDL cholesterol were significantly increased in the LPS-treated group at 16 weeks postpartum (Figure 3). In contrast, control nonpregnant LPS-treated rats did not exhibit increased cholesterol levels (Supplementary Figure S2A). Visceral fat was measured at 16 weeks postpartum. There were no significant differences in omental, mesenteric, parametrial, retroperitoneal, and

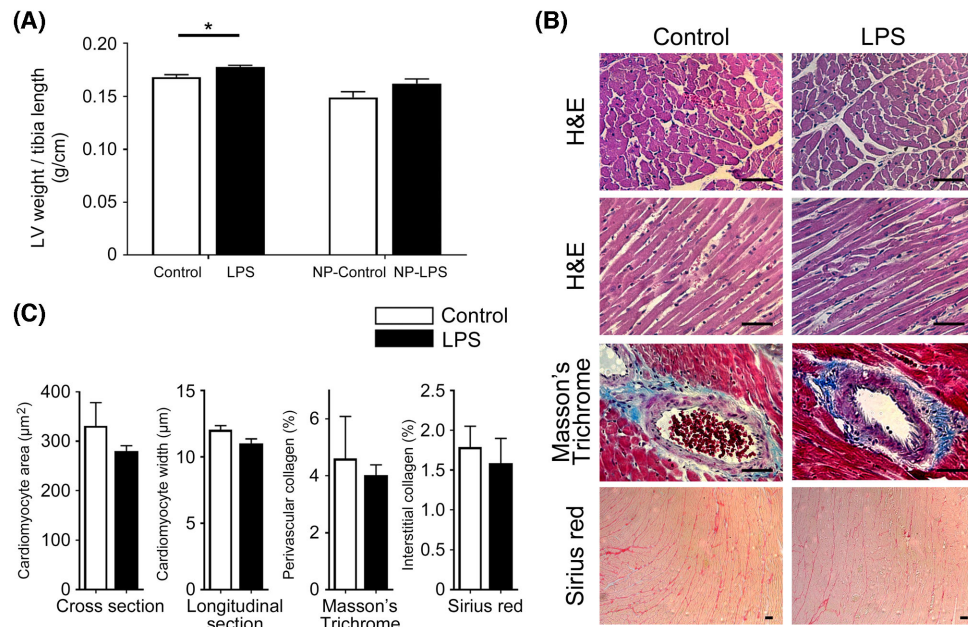


**Figure 1.** Inflammation in pregnancy induces cardiac hypertrophy at 16 weeks postpartum. (A) Left ventricular weights in pregnant and nonpregnant (NP) groups were normalized to tibia length at 16 weeks postpartum (or an equivalent time-frame for nonpregnant rats). (B) Representative images of H&E staining (cross section and longitudinal section), Masson trichrome staining, Sirius red staining of heart tissue. Scale bar = 50  $\mu$ m. (C) Quantitative morphometric analysis of the cardiomyocyte area and width for a single cell. Perivascular collagen fiber deposition was assessed by Masson trichrome staining. Interstitial collagen fiber deposition was assessed by Sirius red staining. Data were analyzed using Student *t*-test or Mann-Whitney test. Data are represented as mean  $\pm$  SEM (n = 6); \**P* < 0.01. LV, left ventricular; H&E, hematoxylin and eosin.

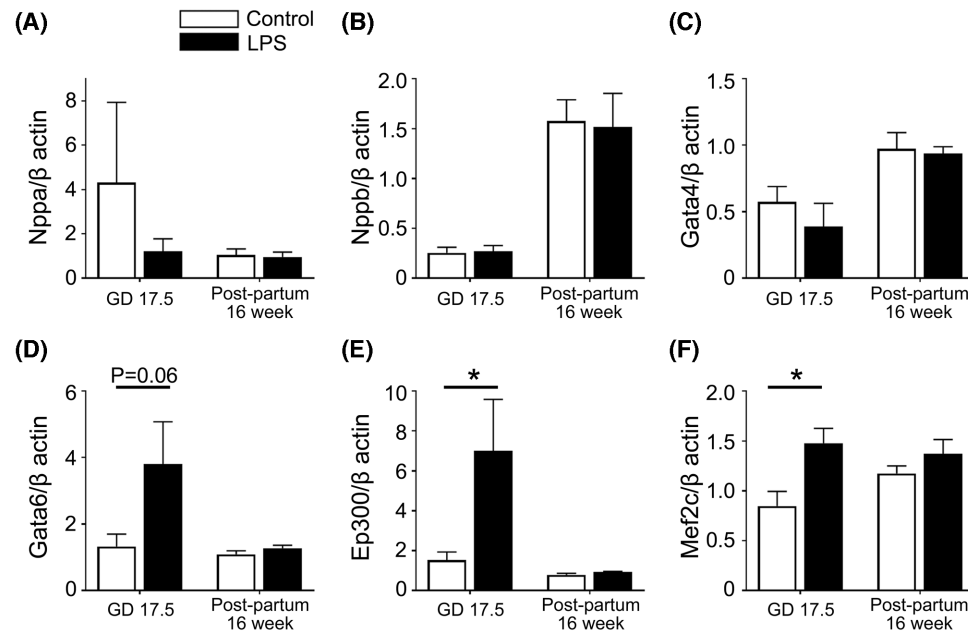


**Figure 2.** Effect of maternal inflammation on cardiac hypertrophy-related gene expression at GD 17.5 and 16 weeks postpartum. Left ventricular mRNA expression of *Nppa*, *Nppb*, *Gata4*, *Gata6*, *Ep300*, and *Mef2c* were measured by qPCR. Data were analyzed using Student *t*-test or Mann-Whitney test. Data are presented as mean  $\pm$  SEM (n = 5~9); \**P* < 0.05. GD, gestational day.

perirenal fat accumulation between the two groups (Supplementary Figure S2B). The rate of body weight gain from GD 13.5–22.5 in LPS-treated rats decreased significantly compared with controls (*P* < 0.01; Supplementary Figure S2C). However, body weight gain from GD 0.5 to postpartum 16 weeks was not significantly differ-

ent in control versus LPS-treated rats (Supplementary Figure S2C). Food intake measured every week after 3 weeks postpartum up to 16 weeks was not significantly different in control versus LPS-treated rats (17.4  $\pm$  0.9 g and 19.3  $\pm$  1.2 g per day at 16 weeks postpartum, respectively, *P* = 0.26; Supplementary Figure S2D). Similarly, there

**Table 1.** Cardiac function: hemodynamic parameters, echocardiography data, and PWV values.

Cardiac function	Control (N = 6)	LPS (N = 6)
<b>Blood pressure</b>		
Mean arterial pressure (mmHg)	122.1 ± 8.3	114.5 ± 6.9
Systolic pressure (mmHg)	147.5 ± 8.9	136.0 ± 7.3
Diastolic pressure (mmHg)	109.4 ± 8.1	103.8 ± 6.7
Pulse pressure (mmHg)	38.1 ± 1.5	32.2 ± 1.3*
Heart rate (bpm)	376 ± 12	392 ± 9.4
<b>Echocardiography</b>		
Ejection fraction (%)	74.4 ± 2.2	74.8 ± 3.8
Fractional shortening (%)	44.7 ± 2.1	45.4 ± 3.6
Cardiac output (ml/min)	71.8 ± 5.3	69.6 ± 5.3
Mitral E/A index	1.75 ± 0.18	1.94 ± 0.11
Myocardial performance (Tei) index	0.494 ± 0.045	0.415 ± 0.031
<b>PWV</b>		
PWV (m/s)	5.73 ± 0.17	5.57 ± 0.14
$\beta$ index	0.86 ± 0.06	0.79 ± 0.02

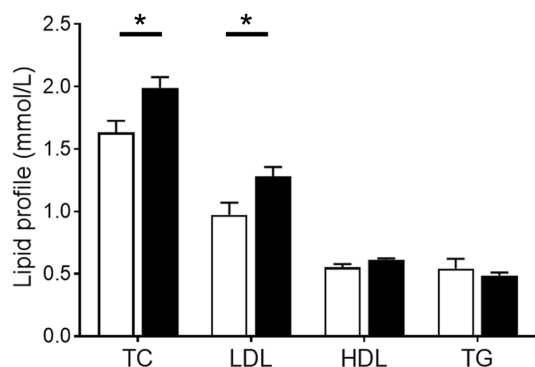
All values are presented as mean ± SEM.

\* $P < 0.05$  versus control.

bpm = beats per minute.

Mitral E/A index = ratio of the early (E) to late (A) ventricular filling velocities.

PWV = pulse-wave velocity.

**Figure 3.** Effect of maternal inflammation on circulating lipids. Serum lipids (TC, LDL, HDL, and TG) were assessed at 16 weeks postpartum. Data were analyzed using Student *t*-test. Data are presented as mean ± SEM ( $n = 6$ ); \* $P < 0.05$ . TC, total cholesterol; LDL, low-density lipoprotein; HDL, high-density lipoprotein; TG, triglycerides.

were no significant differences in fasting glucose levels measured every 4 weeks from delivery to 16 weeks postpartum, and glucose tolerance determined using the IPGTT performed at 16 weeks postpartum (Supplementary Figure S2E and F).

### Effect of maternal inflammation on histone and DNA modifications

We investigated whether the persistent alterations in cardiac parameters and circulating lipids in LPS-treated rats are associated with epigenetic modifications in heart and liver tissues on GD 17.5 and at 16 weeks postpartum. Exposure to LPS during pregnancy resulted in significant increases in the levels of acetylated cardiac histone 3 on GD 17.5 and at 16 weeks postpartum ( $P < 0.05$ ; Figure 4A and B). A trend toward increased lysine 9 monomethylation of cardiac histone 3 (H3K9me) was observed on GD 17.5 and at 16 weeks postpartum ( $P < 0.1$ ; Supplementary Figure S3A). A significant increase in the levels of acetylated histone 4 and a significant decrease in the levels of H3K9me were observed in liver tissues obtained on GD 17.5 ( $P < 0.05$ ; Figure 4C and D; results also shown in Supplementary Figure S3B). No significant differences in the levels of modified histones were observed in kidneys and pancreatic tissues on GD 17.5 or at 16 weeks postpartum (Supplementary Figure S3C and D).

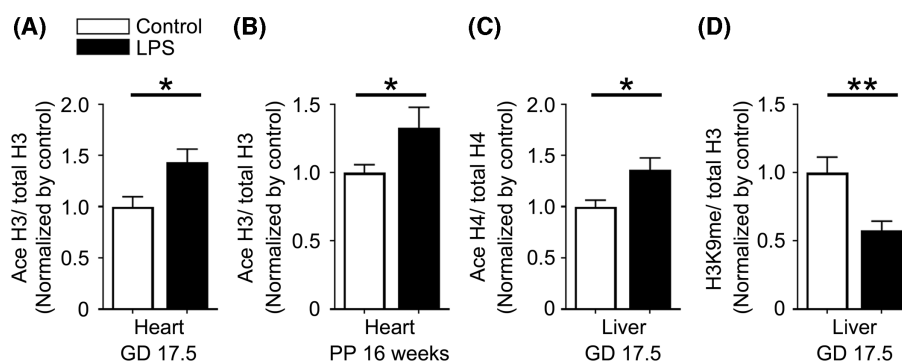
While nonpregnant LPS-treated rats exhibited similar trends in histone modifications, such changes were not statistically significant (Supplementary Figure S3E and F). No significant differences in global DNA methylation in both heart and liver were observed on GD 17.5 and at 16 weeks postpartum (Supplementary Figure S3G and H).

### Effect of maternal inflammation on complete blood count and renal function

No significant differences were observed in the numbers of leukocytes or other blood parameters including erythrocyte counts, hemoglobin, hematocrit, and platelet counts in saline controls versus LPS-treated rats at 16 weeks postpartum (Supplementary Table S2). No significant differences were observed in urine creatinine and urea levels (Supplementary Table S2).

### Discussion

This study investigated whether abnormal inflammation in pregnancy leads to a persistence of risk factors associated with maternal

**Figure 4.** Effect of maternal inflammation on epigenetic modifications. Heart and liver histone modification (acetylation of histone H3 and H4, monomethylation of histone H3K9) was assessed by western blotting on GD 17.5 and 16 weeks postpartum. Data were normalized to the control group. Data were analyzed using Student *t*-test or Mann-Whitney test. Data are presented as mean ± SEM ( $n = 4-10$ ); \* $P < 0.05$ , \*\* $P < 0.01$ . GD, gestational day; PP, postpartum.

cardiovascular disease. The main findings were left ventricular hypertrophy and increased blood cholesterol and LDL levels that persisted long after the pregnancy complicated by inflammation. These risk factors for cardiovascular disease were associated with increased mRNA levels of transcription factors involved in cardiac hypertrophy, measured on GD 17.5, as well as with histone modifications in heart and liver tissues detected at GD 17.5 and at 16 weeks postpartum.

While a link between pregnancy complications associated with aberrant maternal inflammation and increased risk of cardiovascular disease has been well established [1, 2], a causal role for abnormal maternal inflammation in such risk has not been determined. This study provides evidence in support of the concept that a transient exposure to abnormal inflammation can increase the maternal risk of cardiovascular disease in a pregnancy-specific manner, as significant effects of inflammation on left ventricular weight and blood cholesterol and LDL levels were not observed in virgin rats. It is likely that the placenta is a key mediator of the pregnancy-specific effects of inflammation. In our previous study, we demonstrated that a dose of LPS that causes only mild inflammation in nonpregnant rats results in an exaggerated inflammatory response in pregnant rats [29]. There is evidence that under hypoxic or oxidative stress conditions, such as those present in early-onset or severe pre-eclampsia, the placenta releases antiangiogenic and proinflammatory molecules such as sFlt-1 and TNF [40, 41], thereby contributing to the exaggerated systemic inflammation. In our previous study, we observed a rapid increase in circulating TNF levels in pregnant rats following LPS administration [29]; however, despite clear evidence of fetal growth restriction and utero-placental hemodynamic alterations, in a more recent study we did not detect significant increases in circulating sFlt-1 levels in these rats [42]. Thus, it is still unclear whether sFlt-1 has a role in the development of cardiovascular disease risk factors in our rat model.

The timing of LPS administration (GD 13.5–16.5) was chosen based on our previous study in which we demonstrated that a similar protocol resulted in a pre-eclampsia-like condition associated with utero-placental hemodynamic alterations, inhibition of spiral artery remodeling, and an exaggerated systemic inflammatory response [29]. Active remodeling of the spiral arteries in rats normally takes place during this gestational period [43]. Although we have not conducted experiments to determine whether administration of LPS at other gestational days results in similar outcomes, we believe that LPS-induced alterations in utero-placental perfusion (resulting in part from impaired spiral artery remodeling) and the ensuing release of placental proinflammatory molecules are critical for the induction of the pre-eclampsia-like condition.

Several studies have found that abnormal inflammation in nonpregnant rats contributes to epigenetic modifications that alter immune function and inflammatory responses, thereby increasing the risk of cardiovascular and metabolic disease in later life [44, 45]. While methylation of H3K9 is associated with transcriptional silencing, acetylation of histones is associated with transcriptional activation [46]. We detected in LPS-treated rats a significant decrease in the levels of liver H3K9 monomethylation and an increase in the levels of acetylated H3 and H4 in heart and liver tissues, respectively, on GD 17.5, indicating a global shift toward active gene transcription. The effect of LPS on histone modifications was also pregnancy-specific, as nonpregnant rats treated with LPS did not exhibit significant changes in the levels of modified histones compared with saline-treated nonpregnant controls. Further studies are required to fully elucidate the role of histone modifications associated

with pregnancy complications on long-term risk of cardiovascular disease.

Our findings are consistent with retrospective cohort studies on postpartum cardiac function assessed by ultrasound in women with pre-eclampsia. These studies revealed substantial asymptomatic left ventricular dysfunction and hypertrophy 1 year after delivery in preterm pre-eclamptic and term pre-eclamptic women compared with matched controls [10]. Elevated left ventricular mass index (ratio of left ventricular mass to body surface) is strongly correlated with excess adverse cardiovascular events [47] and the risk of recurrent pre-eclampsia [48], as well as with future cardiovascular disease [49]. Although our findings suggest that LPS treatment decreased the area and width of cardiomyocytes, in general, it is known that cardiomyocytes in cardiac hypertrophy exhibit increased size. Given our paradoxical observations, additional investigation is needed to elucidate the effect of LPS-induced inflammation on cardiomyocyte growth.

Cardiac transcription factors, such as those belonging to the GATA family and the myocyte enhancer factor-2 (MEF-2) family, are expressed predominantly in the myocardium. Accumulating data have indicated that these transcriptional activators play significant roles in the regulation of cardiac hypertrophy and remodeling not only during embryogenesis but also during the postnatal period [50]. Hypertrophic stimuli lead to enhanced DNA-binding activity of GATA4, and the transcriptional activity of GATA4 is regulated through interaction with cofactors such as Ep300 and MEF-2 [51, 52]. The transcription factor GATA6 is also important for the regulation of cardiac hypertrophic responses [53, 54]. MEF2C is known to have an essential role in differentiation of myocardial cells and postnatal growth of myocardium [55]. In this study, we found increased expression of *Gata6*, *Ep300*, and *Mef2c* on GD 17.5; however, no significant differences in the levels of these factors were found at 16 weeks postpartum. It is possible that the expression of these cardiac transcription factors is downregulated once hypertrophy is completed.

Our study also revealed significantly increased levels of TC and LDL cholesterol 16 weeks after pregnancy in LPS-treated rats. High levels of LDL cholesterol are strongly linked to an increased risk for cardiovascular disease. Reductions of 1.0 mmol/L in LDL cholesterol levels have been shown to result in up to a 20% decreased risk of cardiovascular events at 1 year [56]. Despite the fact that women who suffer from pre-eclampsia have a substantially higher risk of developing diabetes, our study did not reveal dysfunctions in glucose metabolism in the LPS-treated rats [5, 57].

In this study, aberrant inflammation did not result in detectable blood pressure increases at 16 weeks postpartum when rats were approximately 9 months old. In general, patients who suffer from pre-eclampsia are likely to develop cardiovascular disease or metabolic disease in late midlife or subsequently [1]. It was also reported that women with hypertensive pregnancies have an increased risk of subsequent hypertension after an average of 13.6 years since the index pregnancy [2]. Given that the average life span of female Wistar rats is 2.5–3.0 years [58], it is possible that our rats were too young to exhibit evidence of hypertension and cardiac dysfunction. It is also possible that a combination of predisposing risk factors, and not just inflammation-associated pregnancy complications, contribute to the development of subsequent cardiovascular disease.

Our results are in agreement with a mouse study that showed long-term maternal health effects of pre-eclampsia induced by sFlt-1 injection during pregnancy [59]. In that study, administration of sFlt-1 did not lead to increased maternal blood pressure and

vascular dysfunction at 6 months postdelivery. However, using liquid chromatography–mass spectrometry, the study revealed that sFlt-1 administration was associated with persistent maternal biological alterations associated with cardiovascular disease and atherosclerosis [60]. The authors also concluded that long-term adverse outcomes associated with pre-eclampsia are likely a consequence rather than a mere unmasking of an underlying predisposition.

In this study, we measured blood pressure by inserting a carotid artery catheter under isoflurane anesthesia. Although blood pressure was measured during steady state after the rats reached surgical plane and the depth of anesthesia was comparable in both groups, the effect of anesthesia on blood pressure cannot be ruled out. It is possible, therefore, that differences in blood pressure values between the two groups were underestimated.

We previously showed that the rat model used in this study exhibits various features of pre-eclampsia such as elevated blood pressure, proteinuria, and IUGR [29]. LPS is an endotoxin from gram-negative bacteria, and is widely used in animal experiments to study various inflammation-related diseases. Although inflammation has a role in the development of pre-eclampsia, inflammation induced by LPS may not fully recapitulate the inflammatory processes involved in the development of most human cases of pre-eclampsia. Nevertheless, models of pre-eclampsia involving administration of LPS to pregnant rodents are commonly used and accepted.

In conclusion, this study provides evidence in support of a causal association between aberrant maternal inflammation and the acquisition of risk factors for subsequent cardiovascular disease. Future studies could determine whether management of inflammation during pregnancy represents an effective strategy for reducing the incidence of cardiovascular disease in later life.

## Supplementary data

Supplementary data are available at [BIOLRE](https://doi.org/10.1093/infdis/jny001) online.

**Supplementary Figure S1.** Inflammation in pregnancy induces cardiac hypertrophy at 16 weeks postpartum. Total heart, ventricular, and atrial weight data in LPS-treated and control groups (A) as well as nonpregnant LPS- and saline-treated rats (B) were normalized to tibia length. Data were analyzed using Student *t*-test or Mann–Whitney test. Data are presented as mean  $\pm$  SEM ( $n = 5$ –6); \* $P < 0.05$ , \*\* $P < 0.01$ . LV, left ventricular; RV, right ventricular; LA, left atrium; RA, right atrium.

**Supplementary Figure S2.** Effect of maternal inflammation on circulating lipids, visceral fat accumulation, body weight, food consumption, and glucose metabolism. (A) Serum lipids (total cholesterol, low-density lipoprotein, high-density lipoprotein and triglycerides) in nonpregnant LPS- and saline-treated rats were assessed after 16 weeks. (B) Visceral fat accumulation was assessed at 16 weeks postpartum. Maternal body weight (C) and food consumption (D) were measured weekly. (E) Fasting blood glucose levels were measured every 4 weeks from delivery to postpartum 16 weeks. (F) Intraperitoneal glucose tolerance test was performed at 16 weeks postpartum. Blood glucose levels were assessed after injection of 20% glucose solution (injected at time 0). Data were analyzed using Student's *t*-test, Mann–Whitney test, or repeated-measures two-way ANOVA. Data are presented as mean  $\pm$  SEM ( $n = 5$ –6); \* $P < 0.05$ . TC, total cholesterol; LDL, low-density lipoprotein; HDL, high-density lipoprotein; TG, triglycerides; NP, nonpregnant; GD, gestational day; PP, postpartum.

**Supplementary Figure S3.** Effect of maternal inflammation on epigenetic modifications. Heart, liver, kidney, and pancreas histone modifications (acetylation of histone H3 and H4, monomethylation of histone H3K9) were assessed by western blotting on GD17.5 and 16 weeks postpartum (A–D) as well as in nonpregnant LPS- and saline-treated rats 16 weeks after LPS administration (E and F). Results in this figure showing statistically significant differences are also presented in Figure 3. Data were normalized to control group. Percentage of heart and liver global DNA methylation was assessed on GD 17.5 and 16 weeks postpartum (G and H). Data were analyzed using Student's *t*-test or Mann–Whitney test. Data are presented as mean  $\pm$  SEM ( $n = 4$ –10); \* $P < 0.05$ , \*\* $P < 0.01$ . GD, gestational day; PP, postpartum; NP, nonpregnant.

**Supplementary Table S1.** Primer sequences for qPCR.

**Supplementary Table S2.** Complete blood cell count and renal function at 16 weeks postpartum.

**Supplementary Table S3.** List of Antibodies.

## Acknowledgments

We would like to thank the following individuals: Kim Lavery for performing PWV and measuring blood pressure; Terry Yantian Li for technical support with histology and PCR; Lori Minassian for technical support with PCR; Deborah Harrington and Dr Janine Handforth for technical assistance with CBC data collection; Spencer Barr for technical support with western blot; and Maggie Chasmar for assistance with animal care.

**Conflict of Interest:** The authors have no conflicts of interest to declare in association with this study.

## References

1. Cirillo PM, Cohn BA. Pregnancy complications and cardiovascular disease death: 50-year follow-up of the Child Health and Development Studies pregnancy cohort. *Circulation* 2015; **132**:1234–1242.
2. Marin R, Gorostidi M, Portal CG, Sanchez M, Sanchez E, Alvarez J. Long-term prognosis of hypertension in pregnancy. *Hypertens Pregnancy* 2000; **19**:199–209.
3. Davis EF, Lazdam M, Lewandowski AJ, Worton SA, Kelly B, Kenworthy Y, Adwani S, Wilkinson AR, McCormick K, Sargent I, Redman C, Leeson P. Cardiovascular risk factors in children and young adults born to preeclamptic pregnancies: a systematic review. *Pediatrics* 2012; **129**:e1552–e1561.
4. Yang JJ, Lee SA, Choi JY, Song M, Han S, Yoon HS, Lee Y, Oh J, Lee JK, Kang D. Subsequent risk of metabolic syndrome in women with a history of preeclampsia: data from the Health Examinees Study. *J Epidemiol* 2015; **25**:281–288.
5. Feig DS, Shah BR, Lipscombe LL, Wu CF, Ray JG, Lowe J, Hwee J, Booth GL. Preeclampsia as a risk factor for diabetes: a population-based cohort study. *PLoS Med* 2013; **10**:e1001425.
6. D'Agostino RB, Sr, Pencina MJ, Massaro JM, Coady S. Cardiovascular disease risk assessment: insights from framingham. *Glob Heart* 2013; **8**:11–23.
7. Barker DJ. The origins of the developmental origins theory. *J Intern Med* 2007; **261**:412–417.
8. Barker DJ, Gluckman PD, Godfrey KM, Harding JE, Owens JA, Robinson JS. Fetal nutrition and cardiovascular disease in adult life. *Lancet* 1993; **341**:938–941.
9. Gluckman PD, Hanson MA. The developmental origins of the metabolic syndrome. *Trends Endocrinol Metab* 2004; **15**:183–187.
10. Melchiorre K, Sutherland GR, Liberati M, Thilaganathan B. Preeclampsia is associated with persistent postpartum cardiovascular impairment. *Hypertension* 2011; **58**:709–715.
11. Veerbeek JH, Hermes W, Breimer AY, van Rijn BB, Koenen SV, Mol BW, Franx A, de Groot CJ, Koster MP. Cardiovascular disease risk factors after

- early-onset preeclampsia, late-onset preeclampsia, and pregnancy-induced hypertension. *Hypertension* 2015; 65:600–606.
12. Sibai BM, Mercer B, Sarinoglu C. Severe preeclampsia in the second trimester: recurrence risk and long-term prognosis. *Am J Obstet Gynecol* 1991; 165:1408–1412.
  13. Skjaerven R, Vatten LJ, Wilcox AJ, Ronning T, Irgens LM, Lie RT. Recurrence of pre-eclampsia across generations: exploring fetal and maternal genetic components in a population based cohort. *BMJ* 2005; 331:877.
  14. Mol BW, Roberts CT, Thangaratinam S, Magee LA, de Groot CJ, Hofmeyr GJ. Pre-eclampsia. *Lancet* 2016; 387:999–1011.
  15. Redman CW, Sargent IL. Immunology of pre-eclampsia. *Am J Reprod Immunol* 2010; 63:534–543.
  16. Challis JR, Lockwood CJ, Myatt L, Norman JE, Strauss JF, 3rd, Petraglia F. Inflammation and pregnancy. *Reprod Sci* 2009; 16:206–215.
  17. Redman CW, Sacks GP, Sargent IL. Preeclampsia: an excessive maternal inflammatory response to pregnancy. *Am J Obstet Gynecol* 1999; 180:499–506.
  18. Cotechini T, Graham CH. Aberrant maternal inflammation as a cause of pregnancy complications: a potential therapeutic target? *Placenta* 2015; 36:960–966.
  19. Borzychowski AM, Sargent IL, Redman CW. Inflammation and pre-eclampsia. *Semin Fetal Neonatal Med* 2006; 11:309–316.
  20. Ramma W, Ahmed A. Is inflammation the cause of pre-eclampsia? *Biochem Soc Trans* 2011; 39:1619–1627.
  21. Erez O, Mastrolia SA, Thachil J. Disseminated intravascular coagulation in pregnancy: insights in pathophysiology, diagnosis and management. *Am J Obstet Gynecol* 2015; 213:452–463.
  22. Pijnenborg R, McLaughlin PJ, Vercruysse L, Hanssens M, Johnson PM, Keith JC, Jr, Van Assche FA. Immunolocalization of tumour necrosis factor-alpha (TNF-alpha) in the placental bed of normotensive and hypertensive human pregnancies. *Placenta* 1998; 19:231–239.
  23. Reister F, Frank HG, Heyl W, Kosanke G, Huppertz B, Schroder W, Kaufmann P, Rath W. The distribution of macrophages in spiral arteries of the placental bed in pre-eclampsia differs from that in healthy patients. *Placenta* 1999; 20:229–233.
  24. Haeger M, Unander M, Norder-Hansson B, Tylman M, Bengtsson A. Complement, neutrophil, and macrophage activation in women with severe preeclampsia and the syndrome of hemolysis, elevated liver enzymes, and low platelet count. *Obstet Gynecol* 1992; 79:19–26.
  25. Wang YY, Tawfik O, Wood GW. Endotoxin-induced abortion in mice is mediated by activated fetal macrophages. *J Leukoc Biol* 1998; 63:40–50.
  26. Hayashi M, Hoshimoto K, Ohkura T, Inaba N. Increased levels of macrophage colony-stimulating factor in the placenta and blood in preeclampsia. *Am J Reprod Immunol* 2002; 47:19–24.
  27. Reister F, Frank HG, Kingdom JC, Heyl W, Kaufmann P, Rath W, Huppertz B. Macrophage-induced apoptosis limits endothelial trophoblast invasion in the uterine wall of preeclamptic women. *Lab Invest* 2001; 81:1143–1152.
  28. Laresgoiti-Servitje E, Gomez-Lopez N, Olson DM. An immunological insight into the origins of pre-eclampsia. *Hum Reprod Update* 2010; 16:510–524.
  29. Cotechini T, Komisarenko M, Sperou A, Macdonald-Goodfellow S, Adams MA, Graham CH. Inflammation in rat pregnancy inhibits spiral artery remodeling leading to fetal growth restriction and features of preeclampsia. *J Exp Med* 2014; 211:165–179.
  30. Falcon BJ, Cotechini T, Macdonald-Goodfellow SK, Othman M, Graham CH. Abnormal inflammation leads to maternal coagulopathies associated with placental haemostatic alterations in a rat model of foetal loss. *Thromb Haemost* 2012; 107:438–447.
  31. Rustveld LO, Kelsey SF, Sharma R. Association between maternal infections and preeclampsia: a systematic review of epidemiologic studies. *Matern Child Health J* 2008; 12:223–242.
  32. Sibai BM, Gordon T, Thom E, Caritis SN, Klebanoff M, McNellis D, Paul RH. Risk factors for preeclampsia in healthy nulliparous women: a prospective multicenter study. The National Institute of Child Health and Human Development Network of Maternal-Fetal Medicine Units. *Am J Obstet Gynecol* 1995; 172:642–648.
  33. Wen SW, Xie RH, Tan H, Walker MC, Smith GN, Retnakaran R. Preeclampsia and gestational diabetes mellitus: pre-conception origins? *Med Hypotheses* 2012; 79:120–125.
  34. Pruthi D, Khankin EV, Blanton RM, Aronovitz M, Burke SD, McCurley A, Karumanchi SA, Jaffe IZ. Exposure to experimental preeclampsia in mice enhances the vascular response to future injury. *Hypertension* 2015; 65:863–870.
  35. Staff AC, Redman CW, Williams D, Leeson P, Moe K, Thilaganathan B, Magnus P, Steegers EA, Tsigas EZ, Ness RB, Myatt L, Poston L et al. Pregnancy and long-term maternal cardiovascular health: progress through harmonization of research cohorts and biobanks. *Hypertension* 2016; 67:251–260.
  36. McCabe KM, Booth SL, Fu X, Shobeiri N, Pang JJ, Adams MA, Holden RM. Dietary vitamin K and therapeutic warfarin alter the susceptibility to vascular calcification in experimental chronic kidney disease. *Kidney Int* 2013; 83:835–844.
  37. Fitch RM, Vergona R, Sullivan ME, Wang YX. Nitric oxide synthase inhibition increases aortic stiffness measured by pulse wave velocity in rats. *Cardiovasc Res* 2001; 51:351–358.
  38. Ventura NM, Jin AY, Tse MY, Peterson NT, Andrew RD, Mewburn JD, Pang SC. Maternal hypertension programs increased cerebral tissue damage following stroke in adult offspring. *Mol Cell Biochem* 2015; 408:223–233.
  39. Tung EW, Winn LM. Epigenetic modifications in valproic acid-induced teratogenesis. *Toxicol Appl Pharmacol* 2010; 248:201–209.
  40. Nevo O, Soleymanlou N, Wu Y. Increased expression of sFlt-1 in vivo and in vitro models of human placental hypoxia is mediated by HIF-1. *Am J Physiol Regul Integr Comp Physiol* 2006; 291:R1085.
  41. Hung TH, Charnock-Jones DS, Skepper JN, Burton GJ. Secretion of tumor necrosis factor-alpha from human placental tissues induced by hypoxia-reoxygenation causes endothelial cell activation in vitro: a potential mediator of the inflammatory response in preeclampsia. *Am J Pathol* 2004; 164:1049–1061.
  42. Robb KP, Cotechini T, Allaire C, Sperou A, Graham CH. Inflammation-induced fetal growth restriction in rats is associated with increased placental HIF-1alpha accumulation. *PLoS One* 2017; 12:e0175805.
  43. Caluwaerts S, Vercruysse L, Luyten C, Pijnenborg R. Endovascular trophoblast invasion and associated structural changes in uterine spiral arteries of the pregnant rat. *Placenta* 2005; 26:574–584.
  44. Bayarsaihan D. Epigenetic mechanisms in inflammation. *J Dent Res* 2011; 90:9–17.
  45. Mann DL. Innate immunity and the failing heart: the cytokine hypothesis revisited. *Circ Res* 2015; 116:1254–1268.
  46. Portela A, Esteller M. Epigenetic modifications and human disease. *Nat Biotechnol* 2010; 28:1057–1068.
  47. Tsao CW, Gona PN, Salton CJ, Chuang ML, Levy D, Manning WJ, O'Donnell CJ. Left ventricular structure and risk of cardiovascular events: a framingham heart study cardiac magnetic resonance study. *J Am Heart Assoc* 2015; 4:e002188.
  48. Valensise H, Lo Presti D, Gagliardi G, Tiralongo GM, Pisani I, Novelli GP, Vasapollo B. Persistent maternal cardiac dysfunction after preeclampsia identifies patients at risk for recurrent preeclampsia. *Hypertension* 2016; 67:748–753.
  49. Shahul S, Medvedofsky D, Wenger JB, Nizamuddin J, Brown SM, Bajracharya S, Salahuddin S, Thadhani R, Mueller A, Tung A, Lang RM, Arany Z et al. Circulating antiangiogenic factors and myocardial dysfunction in hypertensive disorders of pregnancy. *Hypertension* 2016; 67:1273–1280.
  50. Spitz F, Furlong EE. Transcription factors: from enhancer binding to developmental control. *Nat Rev Genet* 2012; 13:613–626.
  51. Dai YS, Markham BE. p300 Functions as a coactivator of transcription factor GATA-4. *J Biol Chem* 2001; 276:37178–37185.
  52. Morin S, Charron F, Robitaille L, Nemer M. GATA-dependent recruitment of MEF2 proteins to target promoters. *Embo J* 2000; 19:2046–2055.
  53. van Berlo JH, Elrod JW, van den Hoogenhof MM, York AJ, Aronow BJ, Duncan SA, Molkentin JD. The transcription factor GATA-6 regulates pathological cardiac hypertrophy. *Circ Res* 2010; 107:1032–1040.

54. Liang Q, De Windt LJ, Witt SA, Kimball TR, Markham BE, Molkentin JD. The transcription factors GATA4 and GATA6 regulate cardiomyocyte hypertrophy in vitro and in vivo. *J Biol Chem* 2001; 276: 30245–30253.
55. Xu J, Gong NL, Bodi I, Aronow BJ, Backx PH, Molkentin JD. Myocyte enhancer factors 2A and 2C induce dilated cardiomyopathy in transgenic mice. *J Biol Chem* 2006; 281:9152–9162.
56. Cholesterol Treatment Trialists' (CTT) Collaboration Baigent, C, Blackwell, L, Emberson, J, Holland, LE, Reith, C, Bhala, N, Peto, R, Barnes, EH, Keech, A, Simes, J, Collins, R. Efficacy and safety of more intensive lowering of LDL cholesterol: a meta-analysis of data from 170 000 participants in 26 randomised trials. *Lancet* 2010; 376: 1670–1681.
57. Wang Z, Wang Z, Wang L, Qiu M, Wang Y, Hou X, Guo Z, Wang B. Hypertensive disorders during pregnancy and risk of type 2 diabetes in later life: a systematic review and meta-analysis. *Endocrine* 2017; 55:809–821.
58. Andreollo NA, Santos EF, Araujo MR, Lopes LR. Rat's age versus human's age: what is the relationship? *Arq Bras Cir Dig* 2012; 25:49–51.
59. Bytautiene E, Lu F, Tamayo EH, Hankins GD, Longo M, Kublickiene K, Saade GR. Long-term maternal cardiovascular function in a mouse model of sFlt-1-induced preeclampsia. *Am J Physiol Heart Circ Physiol* 2010; 298:H189–H193.
60. Bytautiene E, Bulayeva N, Bhat G, Li L, Rosenblatt KP, Saade GR. Long-term alterations in maternal plasma proteome after sFlt1-induced preeclampsia in mice. *Am J Obstet Gynecol* 2013; 208:388.e1–388.e10.